2021

COMPARING SCOOP3D AND GIS-TISSA MODELS FOR SLOPE STABILITY ANALYSIS IN IDUKKI, KERALA, INDIA

Stepan Pikul
Michigan Technological University, spikul@mtu.edu

COMPARING SCOOP3D AND GIS-TISSA MODELS FOR SLOPE STABILITY ANALYSIS IN IDUKKI, KERALA, INDIA

By

Stepan Pikul

A THESIS

Submitted in partial fulfillment of the requirements for the degree of

MASTER OF SCIENCE

In Geology

MICHIGAN TECHNOLOGICAL UNIVERSITY

2021

This thesis has been approved in partial fulfillment of the requirements for the Degree of MASTER OF SCIENCE in Geology.

Department of Geological and Mining Engineering and Sciences

Thesis Co-Advisor: *Dr. Thomas Oommen*

Thesis Co-Advisor: *Dr. K.S. Sajinkumar*

Committee Member: *Dr. John Gierke*

Department Chair: *Dr. Aleksey Smirnov*

Table of Contents

List of Figures

Acknowledgements

I would like to thank my committee member, Dr. John Gierke for revising my thesis, and for his class that made the writing of my thesis easier. The co-advisor Dr. K.S. Sajinkumar for supporting me with data from my study area and sharing his ideas.

I would like to express my deepest gratitude to advisor Dr. Thomas Oommen. He never loses patience and encourages me, was sharing his research experience and motivation. For me, he is a great example of a scientist, mentor, and teacher.

I would like to thank to the GMES department for the knowledge I got, and to Brittany Buschell for her help with any questions.

To my family, that missed me, and the support I filled in from them all the time.

To my friends at home and at Michigan Tech (SIIWA) for meeting you.

To the Fulbright program, for giving me this opportunity and experience that will always be with me.

Abstract

Landslides are the most destructive hazard in the mountainous Idukki district in the State of Kerala, India. Therefore, evaluating the possible occurrence of landslides and analyzing the factors that trigger failure is an essential part of a reliable landslide assessment. Physics-based models are commonly used to determine potential landslide susceptible areas in terms of Factor of Safety (FS). Recent years have seen the use of physics-based methods for regional-scale landslide susceptibility analysis using geospatial tools. In this study, we compare two physics-based models using the same data from Idukki. The two models are the Geographic Information System-Tool for Infinite Slope Stability Analysis (GIS-TISSA) that utilizes the infinite slope stability analysis, and the Scoops3D algorithm that uses limit-equilibrium analysis. The significant difference between these two physics-based models is that the GIS-TISSA assumes a shallow failure surface parallel to the slope angle. In contrast, the Scoops3d evaluates deeper rotational failure surfaces. The results from these two physics-based landslide models are critically evaluated with the existing landslide database to verify the validity of these methods for Idukki.

The results show that the GIS-TISSA model is more effective in landslide-prone area mapping, with 41% of the actual landslides identified as unstable. For the Scoops3D, the same output only identifies 16% of the landslides. The GIS-TISSA model matched 87% landslides with the FS values less than 1.7 within unstable-medium stable classes, while the Scoops3D model shows 62% landslides.

1 Introduction

A landslide is the movement of rocks and soils on a sloped surface that can happen in different mechanisms, causing property damage, human fatalities, or ecosystem instability (Highland et al., 2008). For 20 years, from 1995 to 2015, 3876 landslides caused 163,658 deaths and 11,689 injured worldwide (Froude and Petley, 2018). According to Hauge et al. (2019), landslides as natural disasters are the 4th biggest life taker after floods, earthquakes, and storms. In the Asian region, 75% of all spotted landslides worldwide occur, and 15% of these landslides are happening in India (Froude and Petley, 2018). India deals with landslides every year. The annual loss of 400 million US dollars threatens thousands of lives (Thampi et al., 1995). The Geological Survey of India (GSI) reports that 12% of the country's territory is landslide-prone. One of the main susceptible zones in India is the Western Ghats, especially the Idukki district of the State of Kerala. The recent Rajamala landslide on August 7th, 2020, took 62 lives, reported by Kerala Chief Minister (Ani, 2020). Highlands and heavy rainfalls characterize the Idukki district during the monsoon season that influences the stability of slopes. Studies by Abraham et al. (2019) showed that landslide events are more dependent on prolonged rains in Kerala.

Landslide susceptibility modeling is commonly used to estimate the threat of widespread landslide hazards on a large territory. Landslide susceptibility modeling can be divided into quantitative and qualitative approaches. The latter requires detailed inventory mapping of landslides or expert estimation on the site and suffers from subjectivity. The quantitative approach is usually divided into statistical, which needs historical inventory and parameters of landslides, and the geotechnical or physics-based model (Aleotti and

Chowdhury, 1999, Smith et al., 2014, Oommen et al., 2017). To perform statistical modeling, developing accurate inventory can be challenging. A reliable alternative is the physics-based approaches that allow susceptibility estimation. For the physics-based landslide susceptibility approach, geological or geotechnical input data with digital terrain models (DEM) are essential for possible scenario evaluation (Corominas et al., 2013). The physics-based models use the factor of safety (FS) as a characteristic of slope stability. However, there are several physics-based methods. Some of these models are more suitable for shallow slope failures (for example, GIS-TISSA), whereas others are suitable for deep-seated failures (for example, Scoops3D). In most landslide-prone regions, even when one type of landslide is dominated, a combination of shallow and rotational landslides occurs. This is true in Idukki, where studies have shown (Kuriakose et al. 2008) that shallow landslides dominate the landscape, but other types of slope failures also occur in the region. The question in the regional-scale analysis of landslides using the physics-based model is whether to use a GIS-TISSA model or a Scoops3D model for a landscape with different types of landslides? In this study, we address this question by evaluating the applicability of GIS-TISSA and Scoops3D in Idukki with an extensive database of landslides identified to assess the performance of these models. A comparison of GIS-TISSA and the Scoops3D model over a large study area using a high spatial resolution DEM (12.5 m spatial resolution) has not been performed previously. Comparing these models with existing landslides databases might help us understand the major mechanism of landslides in the Idukki district and factors that significantly influence it.

2 Area of study

The Idukki is the second largest district in the State of Kerala and covers 12.9% of the state (5,105.22 km^2) (Figure1). Forests and mountains cover nearly 97% of Idukki, with altitudes from 1200 to 3900 feet above sea level. The terrain slopes up to 80 degrees are typical for this area. The district population is 1,093,156 (AVST) and mainly inhabits valleys, flat areas, and near the main transportation corridors. During the monsoons, 97% of the roads are damaged and blocked by landslides, debris flows, and floods. Most of the Idukki population lives in landslide-prone areas, leading to population vulnerability and household threats due to landslides. In the year 2018, 341 major landslides were reported from 10 districts of Kerala, and 143 of them located in the Idukki district (Gov of Kerala, 2018). Debris flows are also common in Idukki, and the morphological characteristics of the region can explain the high landslide mobility (Kuriakose et al., 2008).

The Western Ghats is the most distinctive mountain range of the Indian peninsula that stretches 1600 km along the coast. The climate condition with monsoon seasons leads to significant weathering of hornblende gneiss, granite gneiss, lateritic soils, and forest loams that consist of the study area. The Western Ghats can be divided by the Gap of Palghat into north and south segments. Shallow landslides are common in the southern part. Rotational and deeper landslides are more frequent in the northeastern part of Western Ghats. The Idukki district belongs to the southern part of Western Ghats, where soil thickness varies from 0.25-5 m and is prone to shallow landslides (Sreekumar, 2009). Besides, this weathered soil with increasing water content decreases its strength, and the annual rainfall is more than 5000 mm (Kuriakose et al., 2008, Jaiswal and van Westen,

2009). Rainfall intensity is higher during June - September caused by the monsoon season. Studies have shown that, in the Idukki district, cumulative rainfalls greater than 70.6 mm within ten days can trigger landslides (Abraham et al., 2019).

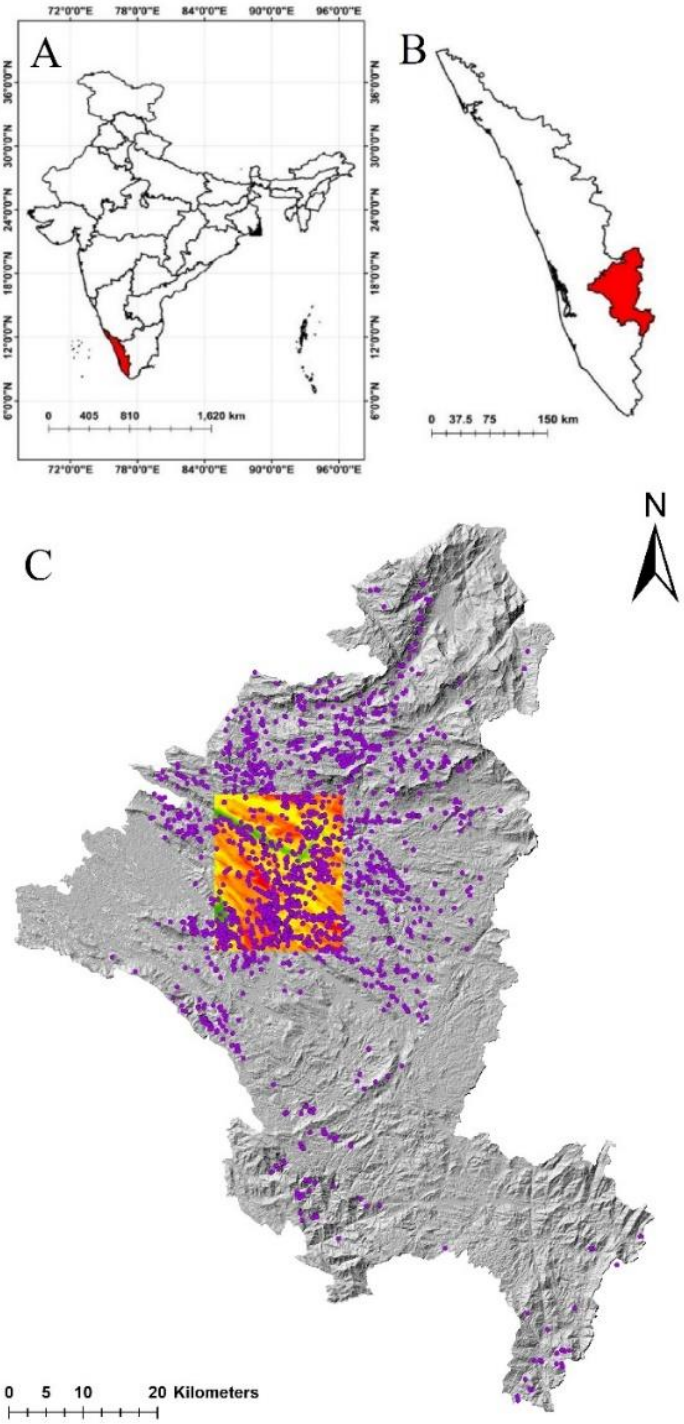

Figure 1. Location map with the study area. a) map of India with the Kerala state; b) Kerala state with the Idukki district; c) The Idukki district with registered landslide dataset and modeled area.

3 Objectives

This study's objective is to perform the GIS-TISSA analysis to perform an infinite slope stability analysis and Scoops 3D stability model by limit-equilibrium analysis. These models represent two main mechanisms of landslides that occur in the area: rotational and shallow landslides. The applicability of these models for regional-scale landslide susceptibility mapping will be analyzed with an existing database that counts near 1000 landslides. No previous study has compared the applicability of these models for a large study area using high spatial resolution DEM (12.5 m).

4 Literature review

The problem of landslides speaks out loudly every year in Idukki. The Idukki, a highland region, is inherently susceptible to landslides. Several different size lineaments cross the district, and the Periyar River originates in the district's upslope and provides the condition for the area's vulnerability to landslides and floods (Vishnu et al., 2019). The Idukki district is known for high landslide activity during the monsoon season. Kuriakose et al. (2008) summarized significant historical landslide events in Kerala and the Idukki district. Study shows that landslides and floods are happening in the area for centuries. However, attention to this area increased last decades with landslides mortality caused by population increase and human activity. Kuriakose et al. (2008) concluded that the Idukki district is prone to shallow landslides on hill slopes >20 degrees based on field observations.

During the monsoons, landslide activation increases, related to increased pore pressure due to intense rainfalls (Kuriakose et al., 2008). The previous studies agree that the increasing events of shallow landslides are associated with deforestation, inefficient land use, and the debris flows resulting from blocking natural drainage systems caused by poor geotechnical decisions (Sajinkumar et al., 2011). Enormous precipitations in summer 2018 led to the most disastrous impact since 1924, with the loss of lives and infrastructure (Kanungo et al., 2020). Post-disaster field observations and landslide mapping gave a detailed vision of primary landslide triggers and recommendations for hazard mitigation. (Sulal and Archana, 2019, Kanungo et al., 2020). Post-disaster field visits concluded that the combination of natural factors and human intervention are reasons for catastrophic losses.

Fieldworks and site visits provided data and materials for laboratory analyses of soil's geotechnical properties for further slope stability modeling (Kuriakose et al., 2008, Sreekumar, 2009).

One of the first slope stability models for the region was developed by Kuriakose et al. (2009) in the Tikovil river basin, which is administratively part of the Idukki and Kottayam districts. In the model, root cohesion as an input parameter has been applied. A physics-based, dynamic, and distributed hydrological model (STARWARS) combined with a probabilistic slope stability model (PROBSTAB) demonstrated slope stability in terms of FS in the Idukki district. Even though the study had insufficient input data, spatial and temporal patterns of landslide-prone areas were generated, indicating slope stability in Idukki depends on few factors like root cohesion, soil depth, and angle of internal friction. A high-resolution Digital Elevation Model (DEM) is no less critical characteristic for shallow landslide prediction (Kuriakose et al., 2009).

A study conducted by Seekumar (2009) focused on hillside slope stability along the road connecting Kottayam and Kumili. This work showed that slope stability estimated using Ordinary and Bishop's methods could describe the mechanics of rotational landslides in the region (basically the Scoops3D method). A stability analysis conducted across a lateritic cross-section at Kumili revealed slopes with conditions close to the threshold of collapsing ($FS < 1.2$) due to moisture content. This decrease in stability can be attributed to the increased piezometric head during heavy rainfall periods (Sreekumar, 2009). Lately, the concepts of multidimensional analysis in the GIS environment in the central

part of the Idukki verified high landslide susceptibly in terms of risk (Abraham and Shaji, 2013, Sajinkumar and Anbazhagan, 2014).

Few more papers tried to demonstrate slope stability through FS in the region. However, the primary input parameter was precipitation data to detect rainfall-triggered landslides. A more detailed landslide study was made in the area of Munnar by Sajinkumar et al. (2017). The local Munnar college site was discovered as a potential landslide-prone area using a vertical electrical sounding method. This method showed that 11 meters of soil near the prior landslide are at high risk of failure. The slope stability analysis based on the one-dimensional infinite slope model proved the area's instability even in dry conditions. Results of this rainfall threshold analysis concluded that landslides happened due to high precipitation amounts across five days (Sajinkumar et al., 2017).

Landslides triggered by rainfall are challenging to predict due to insufficient data from failure locations and precipitation information. One of the methods applied in the study area is the Transient Rainfall Infiltration and Grid-Based Regional slope stability (TRIGRS) by Weidner et al. (2018). This method models slope stability based on a relationship of long-term rainfall and pore pressure. Parameters used in the TRIGRS are a mix of regional data sources, data from remote sensing, and analysis-based parameters of two discovered landslides in the past. The limitation of one-dimensional and TRIGRS models are small area mapping and output with a low-resolution map based on DEM. Besides listed research aimed to classify the study area in terms of stability, more research was done to discover precipitation impact as the main triggering factor in slope instability.

Abraham et al. (2019) developed rainfall thresholds for landslide prediction utilizing three days, ten days, 20 days, 30 days, and 40 days continuous rainfalls as a trigger. Results showed that the possibility of failures increases from 72.12% to 99.56% with increasing rainfall from 3 to 40 days. (Abraham et al., 2019). Lately, by this author, empirical and probabilistic threshold models were improved by the effect of average soil moisture where the soil moisture data was obtained from passive microwave remote sensing (Abraham et al., 2021).

Many landslides in summer 2018 caused by critical heavy rainfall led to a deeper understanding of landslide triggering factors in Idukki. Besides natural factors (i.e., prolonged precipitations, slope parameters, geotechnical soil properties, etc.), the human influence decreases slopes stability. It leads to landslide activation via lack of proper geotechnical measures, slopes cuts, blocking natural drainage, and building's load on soil masses (Sulal and Archana, 2019, Kanungo et al., 2020). Based on landslide sites studied in the State of Kerala, the Landslide Atlas of Kerala was created to include data about the state's risks (Sajinkumar, 2021).

Some of the previous slope stability analyses in Kerala are one-dimensional slope stability analysis, where the slope stability was discovered under dry and wet conditions. (Sajinkumar et al., 2017), Transient Rainfall Infiltration and Grid-based Regional Slope stability (TRIGS) as a tool for modeling slope stability along with the connection between pore pressure and critical rainfall data (Weidner et al., 2018), and GIS Tool for Infinite Slope Stability Analysis (GIS-TISSA) (Escobar-Wolf et al., 2021) that is a ToolBox package of implementation PISA-m algorithms for ArcGIS software was

applied in the Kannur district and showed high correlation with existing landslide database.

5 Methodology

This study aims to compare two models that simulate different landslide mechanisms for the Idukki district in Kerala. The GIS-TISSA and Scoops3D models have significantly different approaches to slope stability computation. GIS-TISSA is the ArcGIS implementation of infinite slope stability analysis and is applicable for shallow landslides modeling. The Scoops3D computes slope stability using limit-equilibrium analysis and is applicable for rotational slides. The performance of these models for the slope stability in Idukki is evaluated here and validated using an existing landslide database.

5.1 GIS-TISSA

The collapse of a thin layer of soil along the surface parallel to the slope is the most common type of landslide, called transitional or shallow landslide (Highland and Bobrowsky, 2008). The slope stability modeling for this type of landslide uses the "infinite slope" model (Naidu et al., 2018). The model shows slope stability as a factor of safety (FS), a ratio of soil shear strength to the shear stress of possible failure surfaces (Zhu et al., 2017). The slope is stable when FS > 1 and unstable when FS < 1. Equation 1 and Fig. 2 shows the parameters used for infinite slope stability analysis (Hammond, 1992).

$$FS = \frac{Cr + Cs[qt + \gamma mD + (\gamma sat - \gamma w)HwD]cos2\beta tan\varphi}{[qt + \gamma mD + (\gamma sat - \gamma w - \gamma m)HwD]sin\beta cos\beta} \quad (1)$$

where:

Cr is the contribution to the soil cohesive strength from the roots (when vegetation is considered)

Cs is the cohesive soil strength

qt is the vegetation weight added to the slope (the surcharge)

γm is the unsaturated (moist, above the phreatic surface) soil unit weight

γsat is the saturated (under the phreatic surface) soil unit weight

γw is the water unit weight, a constant equal to 9810 N/m3 in SI units, or 62.4 lb./ft3 in imperial units

D is the depth of the slip surface

Hw is the height of phreatic surface above slip surface, normalized relative to soil thickness (dimensionless varies from 0 to 1)

β is the terrain slope

ϕ is the internal friction angle of the soil.

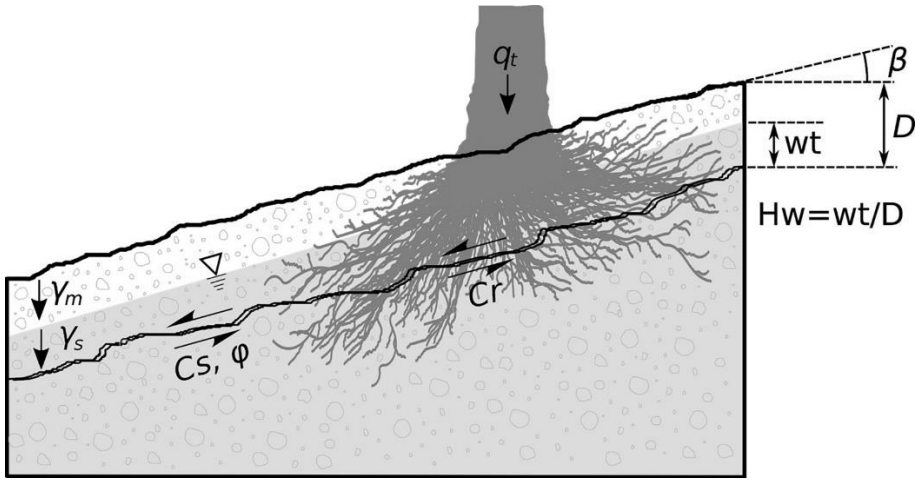

Figure 2. The inputs for the infinite slope stability model (Escobar-Wolf et al., 2021)

Eq.1 does not include uncertainties of input values. Thus, Hammond et al. (1992) suggested a Monte Carlo method to distribute errors and uncertainty calculations from Eq.1. Later, to propagate input uncertainty within the infinite slope model, another approach based on First Order Second Momentum (FOSM) method was applied (Haneberg, 2004). The FOSM method includes two more equations for error calculations in Eq.1. Mean values from the input are used for computing the FS (Eq.2). Assuming that there is no error correlation, the algorithm calculates FS output variance from Eq.3.

$$\underline{FS} = FS(\underline{x}) \tag{2}$$

$\underline{FS}$ is the mean estimation of the factor of safety

FS is the factor of safety calculation function as defined by Eq. (1)

$\underline{x}$ is the set of mean values for the input variables in Eq. (1).

$$(\sigma_{FS})^2 = \sum_i \left(\frac{\partial(FS)}{\partial(x_i)}\right)(\sigma_{xi})^2 \tag{3}$$

σ_{FS} is the standard deviation of FS

$\frac{\partial(FS)}{\partial(x_i)}$ are the partial derivative of FS, given by Eq.1, with respect to any of the input variables *xi*.

σ_{xi} are the estimates of the standard deviation for all the input variables x_i

The mean and standard deviation from Eq. 2, 3 estimates FS of slope stability more reliably, with less computational time. Further, this model was implemented into the software (PISA-m) by Haneberg (2007). The GIS-TISSA is an implementation of the PISA-m algorithm in ESRI® ArcMap software (Escobar-Wolf et al., 2021).

5.2 Scoops3D

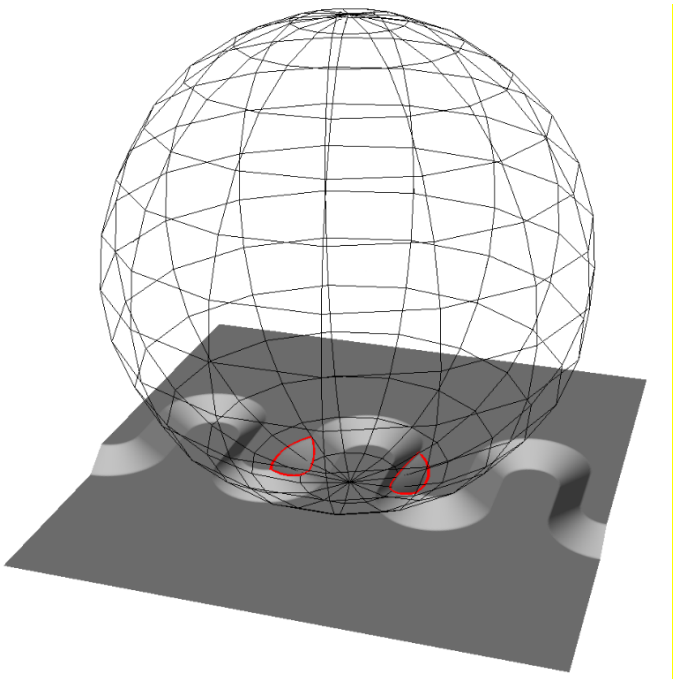

Figure 3. Trial surfaces created by the intersection of the sphere and DEM in two locations. (USGS)

The Scoops3D software was designed by the US Geological Survey (USGS) to calculate the stability of soil masses captured by a significant number of spheres for cutting the surface (Reid, 2015). As a result, it generates trial surfaces by limit-equilibrium analysis, estimates slope stability in three dimensions between the intersection of the DEM surface and potential sliding spheres (Figure 3). It computes the FS for each possible intersection using Bishop's simplified or Fellenius (ordinary) method (Reid, 2015). The ratio of the shear strength to the shear stress defines the FS at the moment of balance, Eq.4. The shear stress is calculated by Mohr-Coulomb failure criterion in Eq.5, where c' is the effective cohesion, φ' is the effective internal friction angle, σ_n is the normal stress, and u is the pore water pressure.

$$FS = \frac{\tau}{s} \tag{4}$$

$$\tau = c' + (\sigma_n - u)tan\varphi' \tag{5}$$

For the moment of equilibrium, the resisting moment is equal to the driving moment. For computing, the FS in Bishop's simplified method normal force must be calculated by the equilibrium force in vertical and horizontal directions (Eq.6, Figure 4).

$$FS = \frac{\sum R_{i,j}\left[c_{i,j}A_{h_{i,j}} + (W_{i,j} - u_{i,j}A_{h_{i,j}})tan\varphi_{i,j}\right]}{\sum W_{i,j}\left(R_{i,j}sin\alpha_{i,j} + k_{eq}e_{i,j}\right)}\frac{1}{m_{\alpha_{i,j}}} \tag{6}$$

Where:

i,j number of column

R represents the radius of a sphere;

A_h represents the horizontal area of a trial slip surface ($A_h = A*cos\varepsilon$);

W represents the weight of the potential failure mass;

α represents the apparent inclination of the sliding direction;

ε represents the intersection angle;

k_{eq} represents the horizontal pseudo acceleration;

e represents the length of the horizontal driving force moment arm.

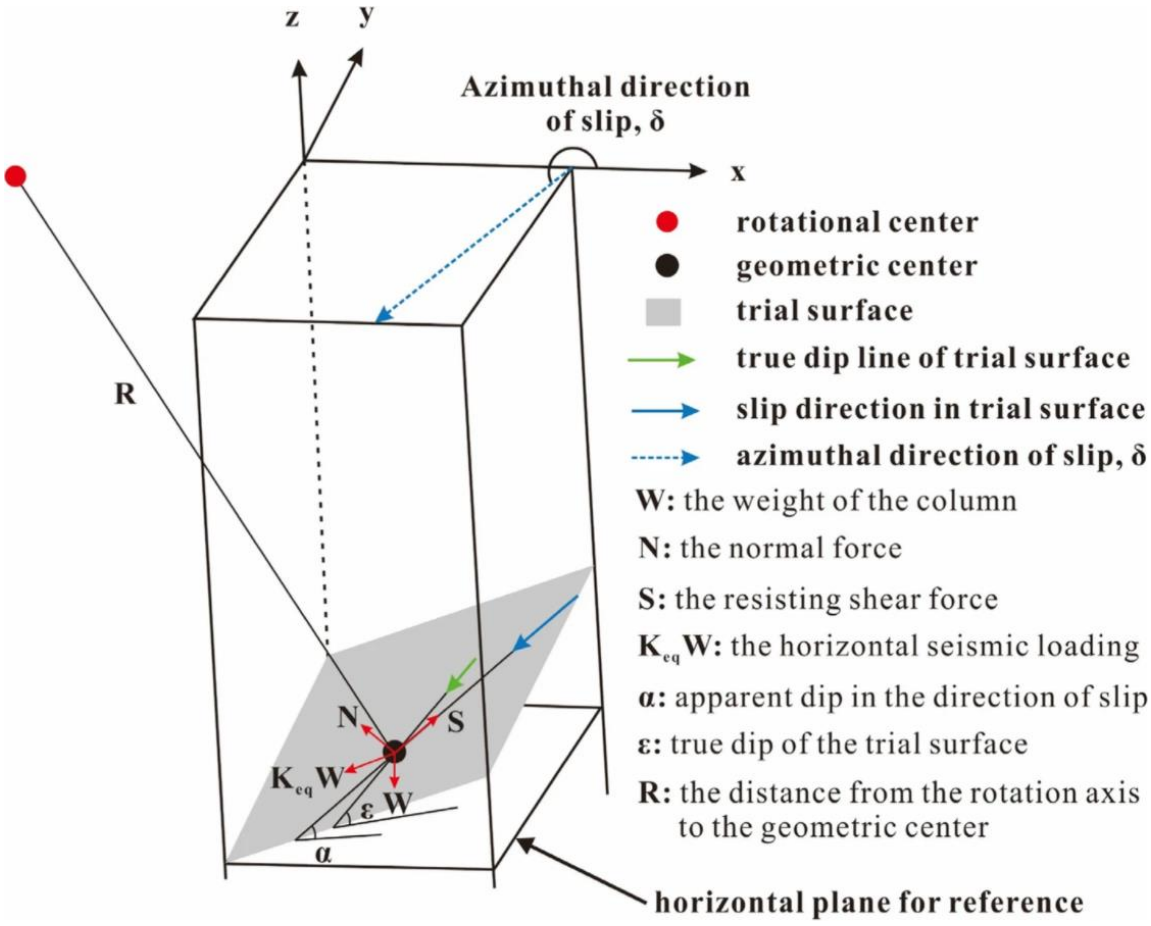

Figure 4. Schematic of forces acting on one column (Zhang and Wang, 2019)

More detailed information about the Scoops3D program can be found in the Scoops3D manual by U.S. Geological Survey (Reid, 2015). Scoops3D software uses few search parameters for controlling the process. These parameters are volume limits, search resolution, and horizontal-vertical distance of search nodes.

Table 1. The input data for Scoops3D

Input data	**Description**
Digital Elevation Model	DEM represents the local topography (ASCII file).
Underground soil layers	A number of soil layers are defined by a set of raster maps of elevations of layer bottoms. The geometry of these soil layers may be irregular. The soil layers may reach the terrain surface or disappear in depth.
Soil parameters (c, ϕ, γ)	Each soil layer has its own soil properties.
Pore-water pressure inputs	Scoops3D provides three different ways to include the pore water pressures on slope stability. No groundwater pressure. Dry underground condition. Pore pressure ratio, r_u. r_u is defined as the ratio of pore pressure to vertical stress at a point. Each soil layer have its own r_u. (3) Piezometric surface. Piezometric surface represents the groundwater surface with vertically hydrostatic heads.
Earthquake loading	Scoops3D includes the horizontal seismic loading using a pseudoacceleration coefficient k_{eq} (-). In the calculation of FS, the k_{eq} multiplied by soil weight represents the horizontal seismic force.

5.3 Model Validation

For classification models, typically, three validation parameters can be used: overall accuracy (OA), precision, and recall. These parameters can be estimated from the confusion matrix. This matrix helps to assess the quality of the classification and evaluates observed classes versus predicted ones. The parameter OA estimates the percentage of accurate classification (Eq.5).

$$OA = (TP + TN)/(Tp + TN + FP + FN) \quad (5)$$

True positive (TP) – the sum of landslide samples correctly predicted; true negative (TN) – sum non-landslide sample correctly predicted; false positive (FP) – the sum of samples non-landslides predicted as landslides; false negative (FN) – the sum of landslides samples predicted as landslides. The parameter precision (Eq.6) estimates how accurate the prediction of a single class and recall (Eq.7) estimates how accurate prediction is based on predicted values (Oommen et al., 2010).

$$precision = TP/(TP + FP) \quad (6)$$

$$recall = TP/(TP + FN) \quad (7)$$

Table 1 Confusion matrix shows where Observed result in Rows and Predicted in Columns

		Observed	
		Yes	**No**
Predicted	**Yes**	TP	FP
	No	FN	TN

To validate the models, 995 landslide locations were used. In the database there are three types of failures: shallow slides - 597 (SS), rockfalls - 38 (RF), and debris flows - 360 (DF). In addition, 1000 random non-landslide points were generated within the modeled area in ArcGIS software within modeled area. FS values were converted to binary outputs (landslides and non-landslides points) using a threshold from both classified models (GIS-TISSA & Scoops3D). The thresholds used for the conversion are 1.0, 1.2, and 1.7.

6 Input parameters

For Scoops3D and GIS-TISSA the digital elevation model is required as an initial input parameter. The DEM with horizontal resolution 12.5 m from the ALOS PULSAR mission was downloaded from the Alaska Satellite Facility website (ASF, 2020) used in the study. A DEM resolution of 12.5 m is the highest available for this area and had not been used for any physics-based modeling of landslide susceptibility of this region before. There are four types of soils in the study area provided by Sajinkumar K.S. (Moderately dry loam, Poorly drained clayey soil, Gravelly loam, and Gravelly loam) (Fig.5).

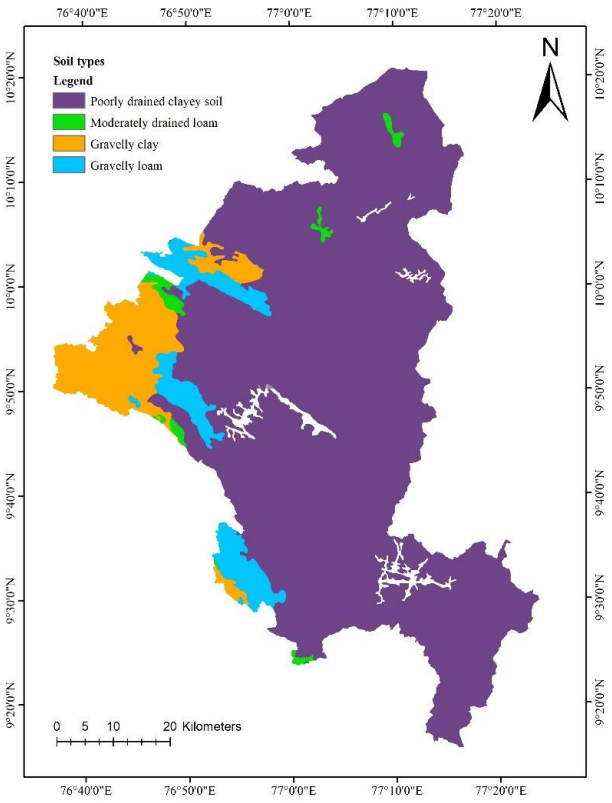

Figure 5.Types of soil in the study area.

Geotechnical parameters of Kerala's soils were analyzed by previous studies (Kuriakose et al., 2009, Weidner et al., 2018). Soil cohesion, unit weight, angle of friction, water table, and soil thickness varied in narrow span and were chosen as a constant value for Scoops3D, for the GIS-TISSA model parameters are used based on papers by Escobar-Wolf et al. (2021) (Table 2 & 3).

Table 2. Input parameters for the Scoops3D model

Input parameter	**Value range**	**Value selected**	**Units**
Cohesion	10,000-18,000	14,000	N/m^2
Internal friction angle	17-23	20	degrees
Unit weight of soil	17,000-19,000	18,000	N/m^2
Saturated unit weight	15,000-19,000	18,000	N/m^2
Soil thickness	0-5	0-5	m
Soil phreatic ratio	0.5	0.5	-

Table 3. Mean and standard deviation soil and tree property values for the GIS-TISSA model

Soil type	Moderately drained loam		Poorly drained clayey soil		Gravelly clay		Gravelly loam	
Property	Mean	STD	Mean	STD	Mean	STD	Mean	STD
Internal friction (degrees)	31	3	24	4	32	2	32	4
Soil cohesion N/m^2	32361	0	14,000	4041	19,000	4,000	26,478	8,492
Depth (m)	5	3.18	5	3.18	5	3.18	5	3.18
Moist unit weight N/m^2	20,787	567	18,165	844	20,459	567	22,752	852
Saturated unit weight N/m^2	16,000	1,500	17,850	1,760	18,296	1,645	15,058	1,331

Soil type Property	Moderately drained loam		Poorly drained clayey soil		Gravelly clay		Gravelly loam	
	Mean	STD	Mean	STD	Mean	STD	Mean	STD
Root cohesion N/m^2	4762	5842	4762	5842	4762	5842	4762	5842
Surcharge N/m^2	1190	481	1190	481	1190	481	1190	481

The GIS-TISSA has the option to include a standard deviation value for each input parameter (Table 3). A fixed value for soil thickness can be used on small-scale, well-discovered areas to study shallow landslides and give reliable results. However, in large areas with low information coverage, the soil thickness survey is costly. A linear equation can define this parameter based on the slope angle (He et al., 2021, Tran et al., 2017). In the study area, the soil thickness is defined as the cosine of the topographic slope, where the maximum thickness 5 m. This equation showed the correlation of soil depth and slope angle from high-resolution imagery at barren rocks (Fig.6) (Weidner et al., 2018). Visual estimate suggested that soil thickness is close to 0 m on slopes with an angle above 40 degrees and can be defined by Eq.6, where *D* is a maximum 5 m depth of soil thickness that reaches zero at slope angle *x* or 40 degree that is equal to 0.698 rad.

$$y = D * \cos(x * 0.44) \quad (6)$$

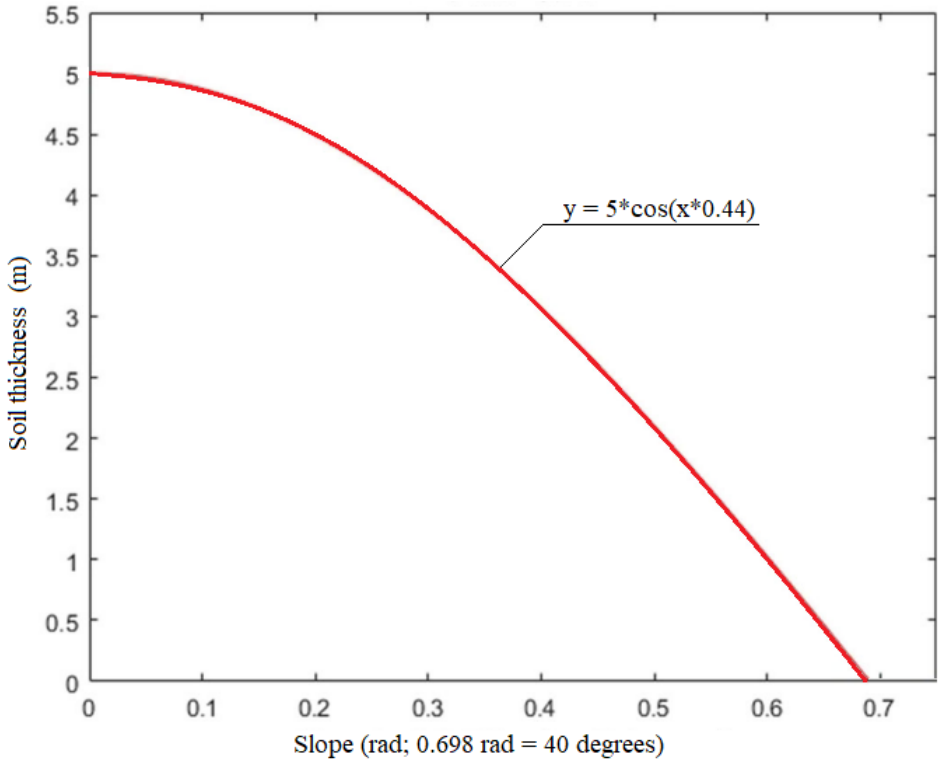

Figure 6. Plot showing the equation used for soil thickness approximation in the study area (Weidner et al., 2018)

To reduce the time-consuming calculation of Scoops3D, a rectangular subset of the study area with the highest density of landslides was chosen within Idukki. There are 995 landslides in the selected area (Figure 1.).

7 Results

In general, the predicted areas with FS less than 1.0 are considered unstable, and FS > 1 are considered stable. To perform more detailed classification, the FS threshold values of 1.0, 1.2, and 1.7 were chosen for both models. The areas with FS less than 1.0 are considered unstable, FS values more than 1 and less than 1.2 are accepted as quasi-stable, FS values between 1.2 and 1.7 considers as medium stable, and more than 1.7 as stable(Table 4) (Escobar-Wolf et al., 2021).

Table 4. Classification of slope stability and instability

Stability classification	Factor of safety	Slope stability class
1	FS < 1	Unstable
2	1 < FS < 1.2	Quasi stable
3	1.2 < FS < 1.7	Medium stable
4	FS > 1.7	Stable

The GIS-TISSA model shows that among 995 landslides in the model area, 41% are located on unstable slope stability class, 18% in the quasi-stable area, and 26.3% belong to the medium stable area. The rest, 12.7%, of landslides are located in the stable zone (Figures 7 & 8). The number of landslides matched with the model's medium and lower stability classes shows a high percentage, and the area classified as unstable covers 20% of the map and matched with 41% of landslides.

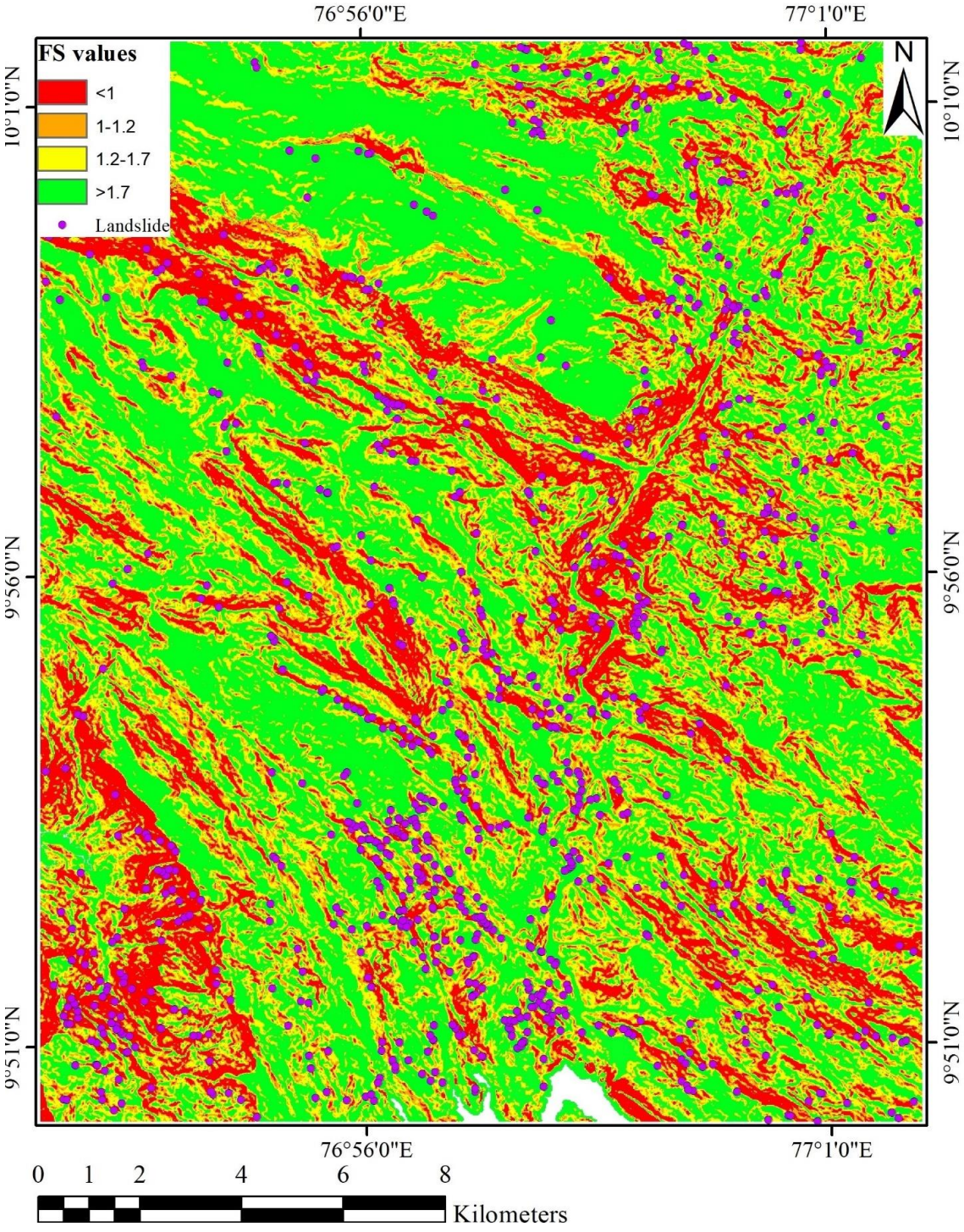

Figure 7. Result of the GIS-TISSA model.

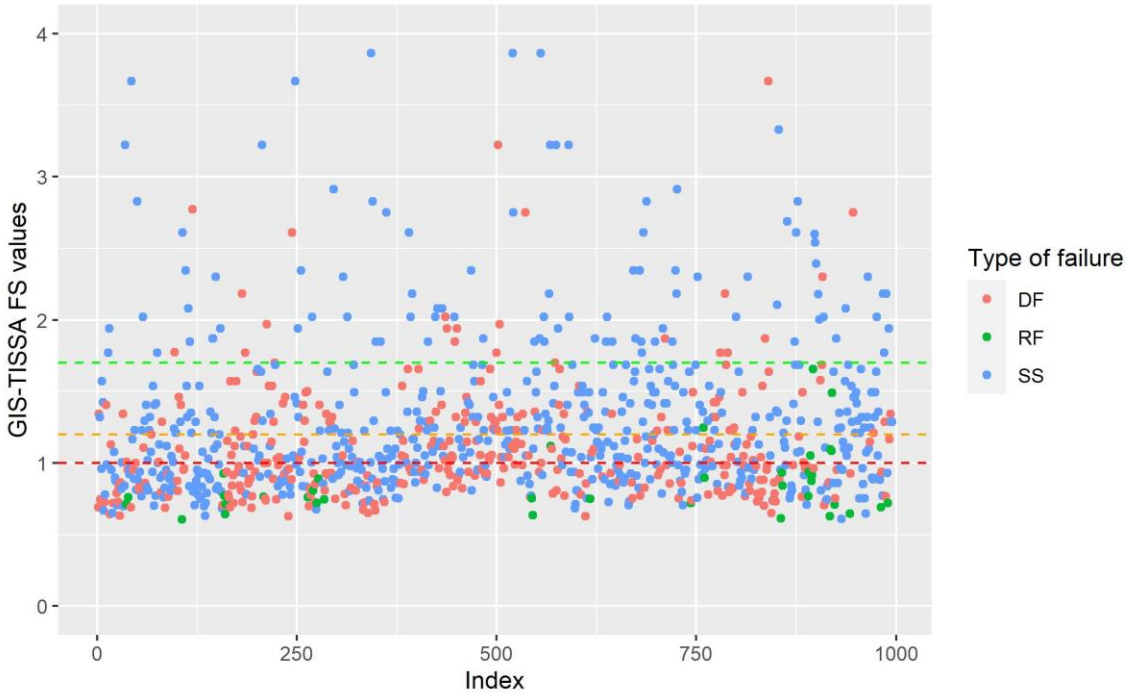

Figure 8. FS values distribution for the GIS-TISSA model (dashed lines represent threshold values of 1.0,1.2, and 1.7, respectively).

The relationship between FS values of landslide points and slope angle in the GIS-TISSA shows that FS can vary for different failures with the same slope angle (Figure 9). It can be explained that input parameters for this model are more flexible in calculations because it accounts for the standard deviation for each parameter like soil cohesion, internal friction, or unit weight. Also, the output result is the mean FS value of each pixel. We have three types of soils present in the modeled area in our situation, each type with different geotechnical parameters. Rock-falls (RF) are more frequent with slope angle increasing, and when slope angle reaches 40 degrees, only two shallow slides (SS) are observed. It supports the idea that soil thickness is related to the slope angle based on Eq.6. Debris Flows (DF) and RF are the main types of failure on weathered high inclined slopes. Some landslide point values are above the major point cloud and belong to the

area with other soil types with higher cohesion parameters, which lead to higher FS. (Figure 9). We observe that the slope angle near 25 degrees, the FS value of the landslides turns to the unstable class. For the quasi unstable class, it is a slope angle near 20 degrees that might support previous studies of shallow landslides that stated that shallow landslides occur on slopes with angles >20 degrees. (Kuriakose et al., 2009).

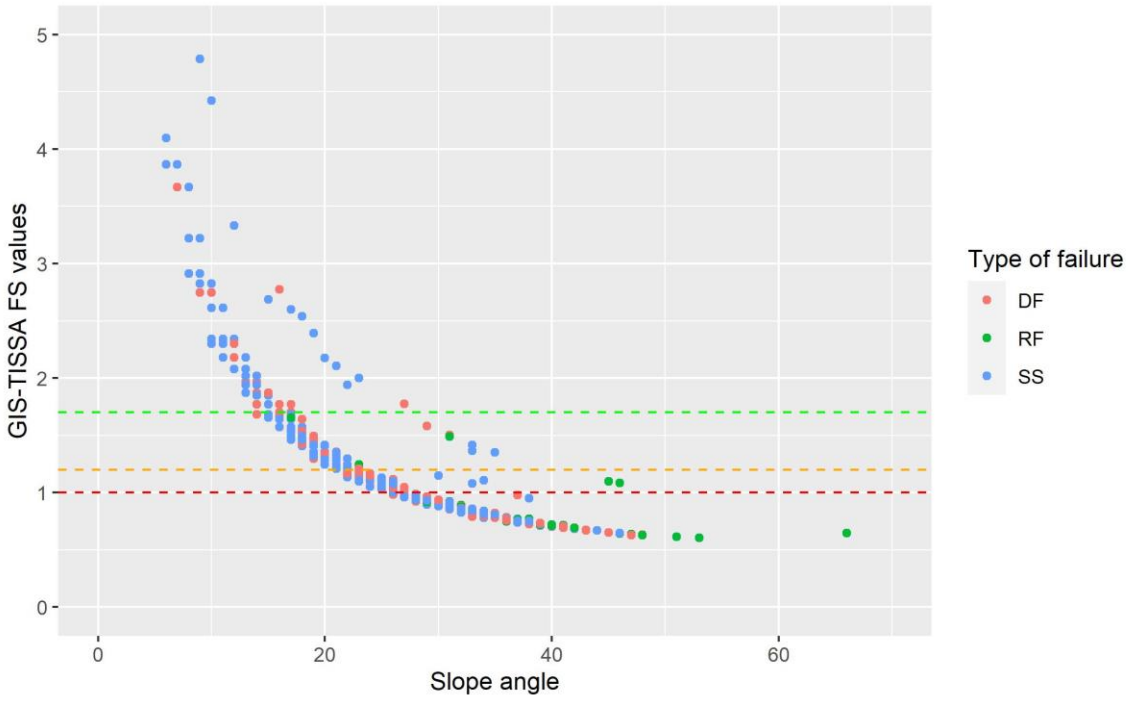

Figure 9. Relation between GIS-TISSA FS values and slope angle with threshold limits.

For the Scoops3D model, only 16.2% of landslides belong to an unstable class. For the quasi-stable -15% of landslides fall in this class, and the medium stable zone - 31.3 % of landslides. Landslides that fall into a stable zone are 37.5% (Figures 10 & 11). An area covered by unstable class is 9%, and the coverage of quasi-stable class is 7%.

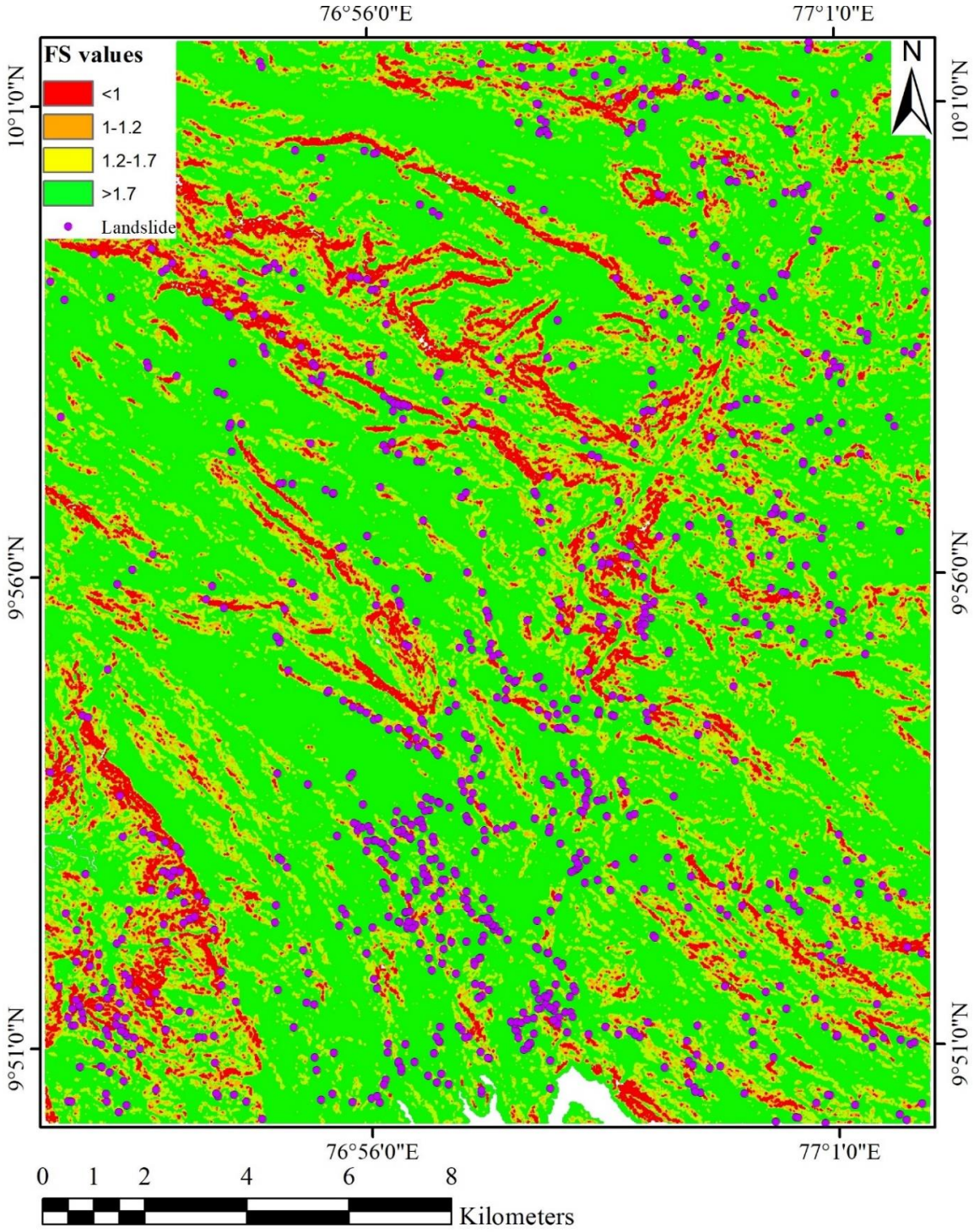

Figure 10. Result of the Scoops3D model.

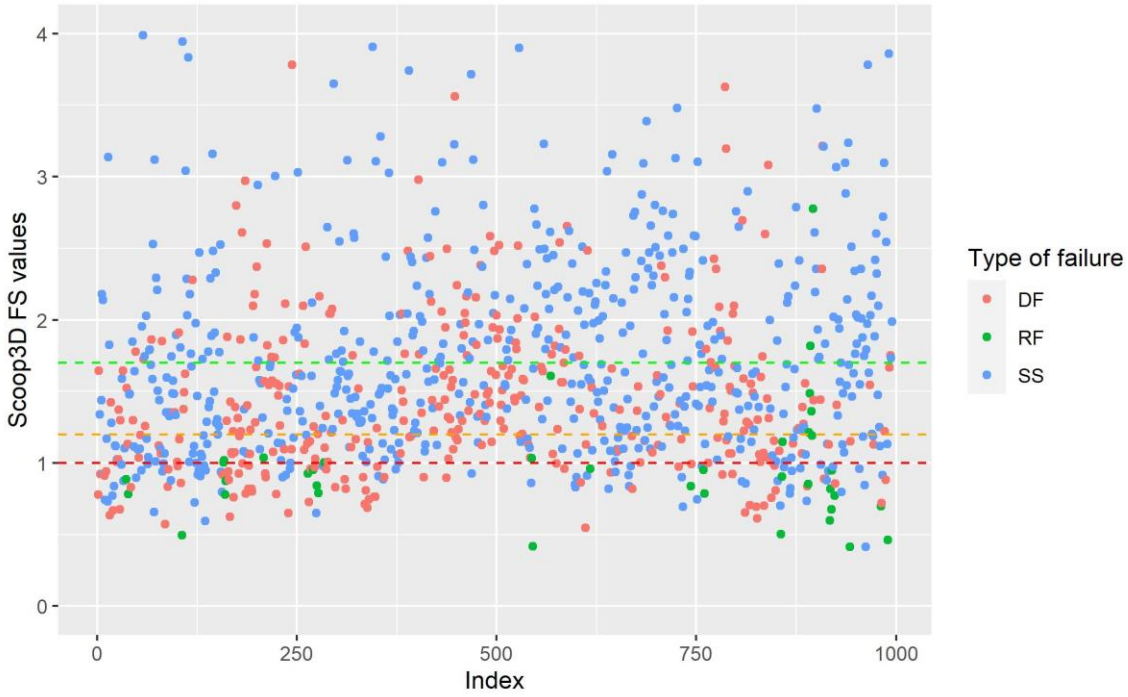

Figure 11. FS values distribution for the Scoops3D model (dashed lines represent threshold values of 1.0, 1.2, and 1.7, respectively).

The relationship between FS values for the Scoops3D model and slope angle shows that slope stability values vary within the same slope angle and that it does not have a strong influence on the FS calculation (Figure 12). For our modeling, the Scoops3D used homogeneous geotechnical parameters. However, the values of landslide volume as an input can change when the program generates trial surfaces and choosing the one with the lowest FS value. The threshold value FS<1 with the lowest slope angle is less than 20 degrees. The average for the intersection of the threshold line and landslides cloud is near 27 degrees.

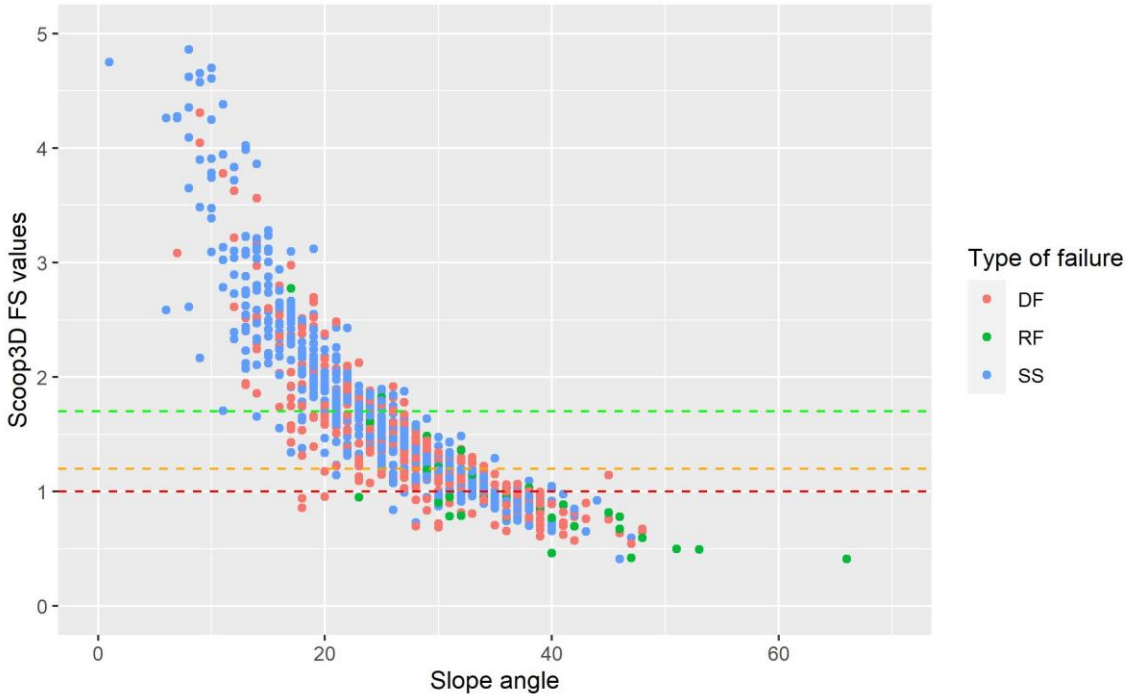

Figure 12. Relation between the Scoops3D FS values and slope angle with threshold limits.

Correlation between the two models shows that FS values for the Scoops3D are higher than for the GIS-TISSA for the same landslide points (Figure 13). It is expected because the GIS-TISSA model covers a larger area in the unstable class, while for the Scoops3D the same class covers a smaller area. Thus, many spatial points are changing class into more stable with higher FS values. Analyzing each type of failure separately, the RF for both models are located in unstable areas. The average slope angle for registered rock falls estimates 37 degrees, which is a reason for low stability values. Debris flow average slope angle is 26 degrees. Thus, FS values are distributed in all stability classes. Shallow landslides FS values spread in wide-angle range with an average slope angle of 23 degrees. The mechanisms that trigger shallow landslide activation are more complex and can include human factors, heavy rainfalls, or soil saturation.

Landslides' location towards slope angle is close to normal distribution for each type of failure (Figure 14). Shallow landslides are located on slopes with lower inclination compared to debris flow and rockfalls. In total, 27% of landslides are located on slopes less than 20 degrees. Comparison of area for each type of failure shows that shallow landslides mostly cover areas near 100-10000 m^2, with a mean of 1360 m^2. While for debris flows, average area values area near 3000 m^2 (Figure 15).

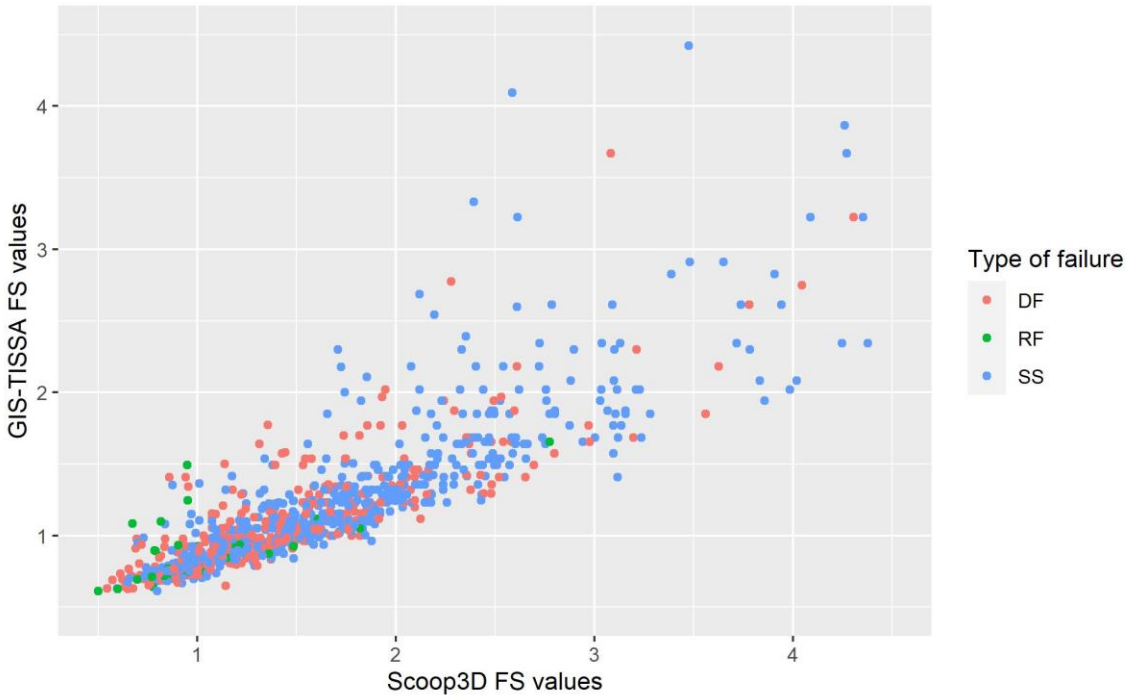

Figure 13. Relation between GIS-TISSA and Scoops3D FS values for landslide point

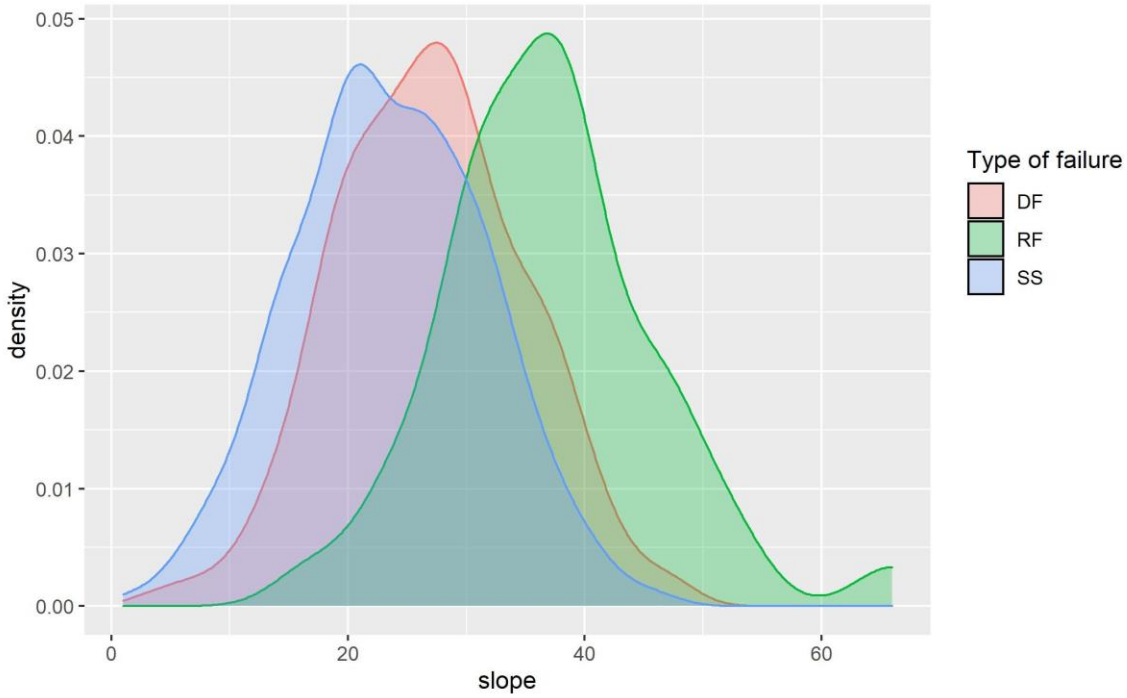

Figure 14. Landslides density distribution on slope angles.

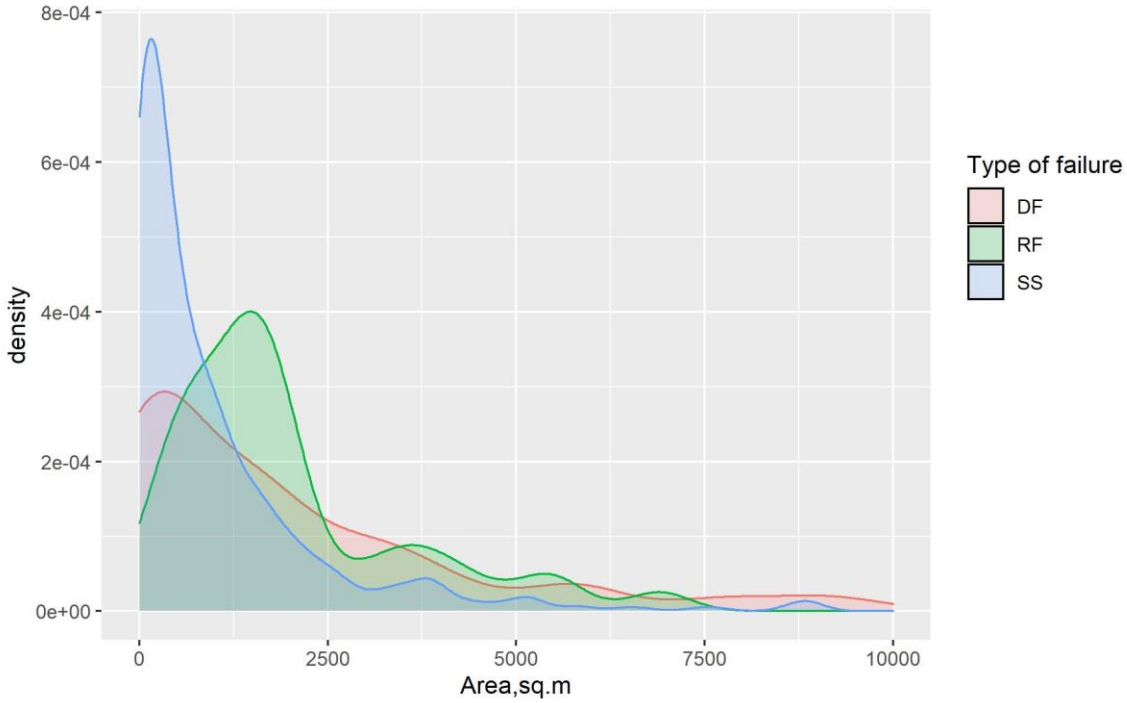

Figure 15. Area of failures density

8 Model validation results

Models validation results show that OA increases with an increasing threshold value (Table 5 & 6). For the GIS-TISSA, it rises from 0.621 for threshold 1.0 to 0.733 for threshold 1.7. The Scoops3D model has lower accuracy, OA= 0.54 for 1.0 threshold and rises to 0.629 for 1.7 thresholds. When the OA parameter shows percentage samples correctly classified, the precision shows the accuracy of predictions, and this parameter is above 0.65 for both models and all threshold values. The recall parameter estimates prediction accuracy according to predicted values. The OA itself cannot show the predictive performance of models. Thus, in model validation, precision and recall parameters were calculated separately for landslides (LS) and non-landslides (NLS) points.

In the case of the GIS-TISSA model, we can see that the model has higher precision for LS and NLS points than the Scoop3D. Precision values for the GIS-TISSA are the highest for the threshold value of 1 and is 0.697, while for the Scoop3D, the highest result is when threshold 1.2 and is 0.689. Also, the recall parameter is higher for the GIS-TISSA model for all threshold values. Based on validation results, for both models the FS=1.2 is an optimal threshold for the prediction of the two classes of LS and NLS points with moderate OA.

Table 5. Models validation results for the GIS-TISSA model

Threshold value/Model	**GIS-TISSA**				
	Recall LS	**Recall NLS**	**Precision LS**	**Precision NLS**	**OA**
FS = 1	0.427	0.185	0.697	0.412	0.621
FS = 1.2	0.599	0.312	0.657	0.367	0.644
FS = 1.7	0.871	0.405	0.682	0.178	0.733

Table 6. Models validation results for the Scoop3D model

Threshold value/Model	**Scoop3D**				
	Recall LS	**Recall NLS**	**Precision LS**	**Precision NLS**	**OA**
FS = 1	0.169	0.09	0.651	0.477	0.54
FS = 1.2	0.314	0.141	0.689	0.444	0.586
FS = 1.7	0.621	0.364	0.63	0.373	0.629

9 Discussion

Despite great results, these models have several limitations that should be considered in further researches. One limitation is the hydrological conditions of the area. On large-scale modeled areas, it is challenging to use proper input for hydrological parameters like the groundwater table level. There is a lack of hydrological data coverage, day-to-day data update, and proper interpolation due to the area's terrain.

Landslides activation is related to monsoon seasons; thus, heavy rainfalls are the no less important trigger that cannot be counted in physical-based modeling by the GIS-TISSA and the Scoop3D models. In the future, these models can be combined with models that are focused on precipitation or can be used for small-scale modeling with accurate rain gauge data.

Based on the results, 13% of failures are located in stable zones for the GIS-TISSA, and 38% for the Scoop3D. Also, 27% of landslides happened on low inclined slopes. The main triggers might be a combination of the human factors, rainfalls amount, hydrological conditions, and other factors that should be referred to understand in next further investigations. In addition, landslides that happened in stable classified areas have uncertainties that our models cannot predict. Revising of threshold values of stability classes could show more accurate results in prediction and matching with a higher percentage of LS points.

Slope stability modeling based on 12.5 m DEM showed detailed results for the study area. However, DEM resolution improvement can be gained through geostatistical methods and applied on small-scaled areas with high landslide density

10 Conclusions

In this work, the GIS-TISSA model was used for infinite slope stability analysis, and Scoops3D was applied to calculate three-dimensional slope stability estimation. DEM with resolution 12.5 m has been used for the first time for slope stability modeling in the study area. As one of the input parameters defining output resolution, it showed more detailed results for both models than previous studies based on SRTM data with a 30 m spatial resolution. Other input parameters of soil's geotechnical properties were chosen based on field observations of other authors and previous studies. For adequate comparison of models, the soil parameters were picked up the constant for the Scoop3D model (Table 2) and the same values for the GIS-TISSA with standard deviations (Table 3).

Comparing the GIS-TISSA and the Scoops3D models showed that the GIS-TISSA was more accurate in landslide slope stability analysis based on the existing database. The GIS-TISSA covered 87% of landslides spot within unstable to medium stable zones. While for the Scoops3D model, coverage is only 62%.

The OA of models increases with increasing a threshold value. The GIS-TISSA shows better prediction results of all types of landslides. The threshold value FS=1.2 shows a satisfactory prediction of LS and NLS for both models.

Analysis of slope angle towards FS values shows that GIS-TISSA landslide point falls into unstable class when slope inclination is more than 20 degrees. This supports previous studies' conclusions; however, 27% of failures happened in areas with lower slope

inclination. According to remote sensing observations of the landslide locations, these failures mainly occur in cultivated lands or near the roads due to human interventions.

Comparing the GIS-TISSA and Scoops3D model indicates that the GIS-TISSA is more applicable for regional-scale landslide susceptibility mapping when multiple landslides types exist within the study area.

Reference List

Abraham, M. T., Pothuraju, D. & Satyam, N. 2019. Rainfall Thresholds for Prediction of Landslides in Idukki, India: An Empirical Approach. *Water,* 11.

Abraham, M. T., Satyam, N., Rosi, A., Pradhan, B. & Segoni, S. 2021. Usage of antecedent soil moisture for improving the performance of rainfall thresholds for landslide early warning. *Catena,* 200.

Abraham, P. B. & Shaji, E. 2013. Landslide hazard zonation in and around Thodupuzha-Idukki-Munnar road, Idukki district, Kerala: A geospatial approach. *Journal of the Geological Society of India,* 82**,** 649-656.

Aleotti, P. & Chowdhury, R. 1999. Landslide hazard assessment: summary review and new perspectives. *Bulletin of Engineering Geology and the Environment,* 58**,** 21-44.

Corominas, J., van Westen, C., Frattini, P., Cascini, L., Malet, J. P., Fotopoulou, S., Catani, F., Van Den Eeckhaut, M., Mavrouli, O., Agliardi, F., Pitilakis, K., Winter, M. G., Pastor, M., Ferlisi, S., Tofani, V., Hervás, J. & Smith, J. T. 2013. Recommendations for the quantitative analysis of landslide risk. *Bulletin of Engineering Geology and the Environment*.

Escobar-Wolf, R., Sanders, J. D., Vishnu, C. L., Oommen, T. & Sajinkumar, K. S. 2021. A GIS tool for infinite slope stability analysis (GIS-TISSA). *Geoscience Frontiers,* 12**,** 756-768.

Froude, M. J. & Petley, D. N. 2018. Global fatal landslide occurrence from 2004 to 2016. *Natural Hazards and Earth System Sciences,* 18**,** 2161-2181.

Hammond, C. 1992. *Level I stability analysis (LISA) documentation for version 2.0*, US Department of Agriculture, Forest Service, Intermountain Research Station.

Haneberg, W. C. 2004. A rational probabilistic method for spatially distributed landslide hazard assessment. *Environmental & engineering geoscience,* 10**,** 27-43.

He, J., Qiu, H., Qu, F., Hu, S., Yang, D., Shen, Y., Zhang, Y., Sun, H. & Cao, M. 2021. Prediction of spatiotemporal stability and rainfall threshold of shallow landslides using the TRIGRS and Scoops3D models. *Catena,* 197.

Highland, L. M. & Bobrowsky, P. 2008. The Landslide Handbook—

A Guide to Understanding Landslides : Reston,
Virginia. *Book*, 129.

Jaiswal, P. & van Westen, C. J. 2009. Estimating temporal probability for landslide initiation along transportation routes based on rainfall thresholds. *Geomorphology,* 112**,** 96-105.

Kanungo, D. P., Singh, R. & Dash, R. K. 2020. Field observations and lessons learnt from the 2018 landslide disasters in Idukki District, Kerala, India. *CURRENT SCIENCE,* 119**,** 1797.

Kuriakose, S. L., Sankar, G. & Muraleedharan, C. 2008. History of landslide susceptibility and a chorology of landslide-prone areas in the Western Ghats of Kerala, India. *Environmental Geology,* 57**,** 1553-1568.

Kuriakose, S. L., van Beek, L. P. H. & van Westen, C. J. 2009. Parameterizing a physically based shallow landslide model in a data poor region. *Earth Surface Processes and Landforms,* 34**,** 867-881.

Naidu, S., Sajinkumar, K. S., Oommen, T., Anuja, V. J., Samuel, R. A. & Muraleedharan, C. 2018. Early warning system for shallow landslides using rainfall threshold and slope stability analysis. *Geoscience Frontiers,* 9**,** 1871-1882.

Oommen, T., Baise, L. & Asce, M. 2010. Validation and Application of Empirical Liquefaction Models. *Journal of Geotechnical and Geoenvironmental Engineering,* 136.

Oommen, T., Cobin, P. F., Gierke, J. S. & Sajinkumar, K. S. 2017. Significance of variable selection and scaling issues for probabilistic modeling of rainfall-induced landslide susceptibility. *Spatial Information Research,* 26**,** 21-31.

Reid, M. E., Christian, S.B., Brien, D.L., and Henderson, S.T. 2015. *Scoops3D—Software to analyze 3D slope stability throughout a digital landscape: U.S. Geological Survey Techniques and Methods,*.

Sajinkumar, K. S. & Anbazhagan, S. 2014. Geomorphic appraisal of landslides on the windward slope of Western Ghats, southern India. *Natural Hazards,* 75**,** 953-973.

Sajinkumar, K. S., Anbazhagan, S., Pradeepkumar, A. P. & Rani, V. R. 2011. Weathering and landslide occurrences in parts of Western Ghats, Kerala. *Journal of the Geological Society of India,* 78**,** 249.

Sajinkumar, K. S., Asokakumar, M. R., Sajeev, R. & Venkatraman, N. V. 2017. A Potential Headward Retreat Landslide Site at Munnar, Kerala. *Journal of the Geological Society of India,* 89**,** 183-191.

Sajinkumar, K. S., Oommen, T. 2021. Landslide Atlas of Kerala. GSI Publications, 7(1).

Smith, D. M., Oommen, T., Bowman, L. J., Gierke, J. S. & Vitton, S. J. 2014. Hazard assessment of rainfall-induced landslides: a case study of San Vicente volcano in central El Salvador. *Natural Hazards,* 75**,** 2291-2310.

Sreekumar, S. 2009. Techniques for slope stability analysis: Site specific studies from Idukki district, Kerala. *Journal of the Geological Society of India,* 73**,** 813-820.

Sulal, N. & Archana, K. 2019. Note on post disaster studies for landslides occurred in june 2018 at Idukki District, Kerala. *Geological Survey of India, Thiruvananthapuram*.

Thampi, P., Mathai, J. & Sankar, G. A regional evaluation of landslide prone areas in the Western Ghats of Kerala. national seminar on landslides in Western Ghats, 1995. 29-30.

Tran, T. V., Alvioli, M., Lee, G. & An, H. U. 2017. Three-dimensional, time-dependent modeling of rainfall-induced landslides over a digital landscape: a case study. *Landslides,* 15**,** 1071-1084.

Vishnu, C. L., Sajinkumar, K. S., Oommen, T., Coffman, R. A., Thrivikramji, K. P., Rani, V. R. & Keerthy, S. 2019. Satellite-based assessment of the August 2018 flood in parts of Kerala, India. *Geomatics, Natural Hazards and Risk,* 10**,** 758-767.

Weidner, L., Oommen, T., Escobar-Wolf, R., Sajinkumar, K. S. & Samuel, R. A. 2018. Regional-scale back-analysis using TRIGRS: an approach to advance landslide hazard modeling and prediction in sparse data regions. *Landslides,* 15**,** 2343-2356.

Zhu, F., Zhang, W. & Sun, M. 2017. A New Calculation Method for the Soil Slope Safety Factor. *Mathematical problems in engineering,* 2017**,** 1-6.